Designing shielded radio-frequency phased-array coils for magnetic resonance imaging*

Xu Wen-Long(徐文龙)[a)†], Zhang Ju-Cheng(张鞠成)[a)], Li Xia(李 霞)[a)b)], Xu Bing-Qiao(徐冰俏)[a)], and Tao Gui-Sheng(陶贵生)[a)b)]

[a)] *Department of Biomedical Engineering, China Jiliang University, Hangzhou* 310018, *China*
[b)] *Department of Biomedical Engineering, Zhejiang University, Hangzhou* 310027, *China*

(Received 26 May 2012; revised manuscript received 24 October 2012)

In this paper, an approach to the design of shielded radio-frequency (RF) phased-array coils for magnetic resonance imaging (MRI) is proposed. The target field method is used to find current densities distributed on primary and shield coils. The stream function technique is used to discretize current densities and to obtain the winding patterns of the coils. The corresponding highly ill-conditioned integral equation is solved by the Tikhonov regularization with a penalty function related to the minimum curvature. To balance the simplicity and smoothness with the homogeneity of the magnetic field of the coil's winding pattern, the selection of a penalty factor is discussed in detail.

Keywords: active shield, phased-array coil, radio-frequency coil, magnetic resonance imaging

PACS: 02.30.Zz, 41.20.–q, 41.20.Gz, 84.32.Hh **DOI:** 10.1088/1674-1056/22/1/010203

1. Introduction

Magnetic resonance imaging (MRI) is one of the most important noninvasive imaging methods for clinical diagnosis.[1,2] The basic principle of MRI is that the hydrogen nuclei within the human body in a strong, static magnetic field resonate at a radio frequency (RF) (Larmor frequency) that is proportional to the static field strength.[3] Radio-frequency coils operating at the Larmor radio frequency are placed near and around the patient (animal) to excite and receive the MR signals from the hydrogen nuclei.[4] These signals are spatially encoded by gradient coils and digitally processed to form MR images. The target field method, first proposed by Turner, is frequently used in the design of RF coils.[5–8] A possible limitation of this inverse method[9–12] is that it assumes coils of notionally infinite length. To overcome the extra error introduced by the assumption, finite length coils can be designed without approximation by expanding the current density in a Fourier series.[13] The ill-conditioned integral equation is properly solved with a regularization strategy,[14–16] in which penalty functions including minimum power,[17] minimum inductance,[18,19] minimum stored energy,[20] and minimum curvature[21] are applied.

To achieve a better signal-to-noise ratio (SNR), the surface coils are used, although the RF magnetic field (B1) in the specified imaging region of MRI produced by volume RF coils is much more homogeneous than that produced by surface coils.[22] Usually, RF phased-array coils are composed of a number of spatially tightly arranged coils, which can cover a larger volume than that of each single receiver coil.[23] When RF fields impinge on the gradient and shim coils, numerous interactions occur, which can degrade the performance of the RF coils, resulting in lower Q factors and imaging quality degradations. With the increasing main magnetic field, this negative effect becomes unacceptable. Therefore, a shield coil is needed to reduce or eliminate the interactions between the RF coil and the gradient and shim coils.[3,21,24,25]

The target field method proposed for designing unshielded and shielded RF coils introduces a set of Fourier coefficients and needs a large scale of numerical calculations.[8,21] Meanwhile, the corresponding magnetic field induced by the coil designed with a minimum curvature penalty function in the specified imaging region is highly unsatisfactory. The penalty factor determines the accuracy of the solution and the complexity of coil windings. Hence, the selection of the penalty factor is important for finding simple winding patterns with high precision. However, in the literature,[8,21,25] it is not discussed in detail. The inverse method for designing unshielded RF coils[25] is extended to the design of shielded phased-array RF coils and the selection of the penalty factor in this research.

2. Methodology

A sketch map of a cylindrical shielded RF head coil system is shown in Fig. 1. The primary and the shield coils lie coaxially with the z axis, and unknown currents are distributed on the surfaces of the coils, which generate a desired homoge-

*Project supported by the National Nature Science Foundation of China (Grant No. 30900332), Grant of General Administration of Quality Supervision Inspection and Quarantine of China (Grant No. 201210079), the Program for Science and Technology Department of Zhejiang Province, China (Grant Nos. 2010C14010 and 2010C33172), and the Natural Science Foundation of Zhejiang Province, China (Grant No. Y2090966).

†Corresponding author. E-mail: wenlongxu@sina.com

© 2013 Chinese Physical Society and IOP Publishing Ltd

neous magnetic field in a diameter of spherical volume (DSV) and screens magnetic fields out of the shield coil (OUT). Assume the length and radius of the primary coil are $2L$ and a, and the length and radius of the shield coil are $2sL$ and b, respectively. The radius of DSV is c_1. The radius and length of OUT are c_2 and $2tL$, respectively.

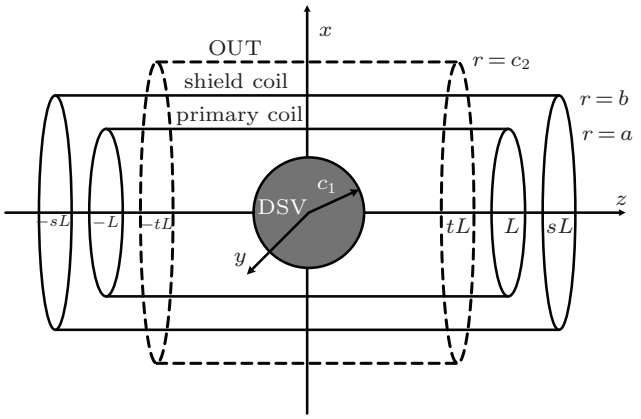


Fig. 1. Sketch map of shielded head coil system.

Based on the Biot–Savart integral expression, the magnetic field vector at any field point can be obtained as

$$\boldsymbol{H}(\boldsymbol{r}) = \frac{1}{2\pi}\iint_S \mathrm{e}^{-\mathrm{i}\alpha R}\left(\frac{\mathrm{i}\alpha}{R^2}+\frac{1}{R^3}\right)(\boldsymbol{r}'-\boldsymbol{r})\times\boldsymbol{j}(\boldsymbol{r}')\,\mathrm{d}S, \quad (1)$$

where $\alpha = \omega\sqrt{\mu_0\varepsilon_0}$, in which angular frequency ω relates to the Larmor frequency, μ_0 represents the permeability of vacuum, and ε_0 represents the permittivity of vacuum; $\boldsymbol{r}$ denotes the position vector of a field point external to the coil; $\boldsymbol{r}'$ represents a source point on the coil surface; $R = |\boldsymbol{r}'-\boldsymbol{r}|$ is the distance between source point $\boldsymbol{r}$ and field point $\boldsymbol{r}'$, and $\boldsymbol{j}(\boldsymbol{r}')$ is the unknown current density distributed on the coil.

Then the y components of the induced magnetic field in the DSV and the OUT can be written as

$$\begin{aligned}
&H_y^{\mathrm{DSV}}(\theta,z)\\
&= -\frac{a}{2\pi}\int_0^{2\pi}\int_{-L}^{L}[(a\cos\theta'-\sqrt{c_1^2-z^2}\cos\theta)j_z^{\mathrm{P}}(\theta',z')\\
&\quad+(z'-z)\sin\theta' j_\theta^{\mathrm{P}}(\theta',z')]\\
&\quad\times\mathrm{e}^{-\mathrm{i}\alpha R_{\mathrm{p}}^{\mathrm{DSV}}}\left(\frac{\mathrm{i}\alpha}{(R_{\mathrm{p}}^{\mathrm{DSV}})^2}+\frac{1}{(R_{\mathrm{p}}^{\mathrm{DSV}})^3}\right)\mathrm{d}z'\,\mathrm{d}\theta'\\
&\quad-\frac{b}{2\pi}\int_0^{2\pi}\int_{-sL}^{sL}[(b\cos\theta'-\sqrt{c_1^2-z^2}\cos\theta)j_z^{S}(\theta',z')\\
&\quad+(z'-z)\sin\theta' j_\theta^{S}(\theta',z')]\\
&\quad\times\mathrm{e}^{-\mathrm{i}\alpha R_{\mathrm{s}}^{\mathrm{DSV}}}\left(\frac{\mathrm{i}\alpha}{(R_{\mathrm{s}}^{\mathrm{DSV}})^2}+\frac{1}{(R_{\mathrm{s}}^{\mathrm{DSV}})^3}\right)\mathrm{d}z'\,\mathrm{d}\theta', \qquad (2)\\
&H_y^{\mathrm{OUT}}(\theta,z)\\
&= -\frac{a}{2\pi}\int_0^{2\pi}\int_{-L}^{L}[(a\cos\theta'-c_2\cos\theta)j_z^{\mathrm{P}}(\theta',z')\\
&\quad+(z'-z)\sin\theta' j_\theta^{\mathrm{P}}(\theta',z')]\\
&\quad\times\mathrm{e}^{-\mathrm{i}\alpha R_{\mathrm{p}}^{\mathrm{OUT}}}\left(\frac{\mathrm{i}\alpha}{(R_{\mathrm{p}}^{\mathrm{OUT}})^2}+\frac{1}{(R_{\mathrm{p}}^{\mathrm{OUT}})^3}\right)\mathrm{d}z'\,\mathrm{d}\theta'\\
&\quad-\frac{b}{2\pi}\int_0^{2\pi}\int_{-sL}^{sL}[(b\cos\theta'-c_2\cos\theta)j_z^{S}(\theta',z')\\
&\quad+(z'-z)\sin\theta' j_\theta^{S}(\theta',z')]\\
&\quad\times\mathrm{e}^{-\mathrm{i}\alpha R_{\mathrm{s}}^{\mathrm{OUT}}}\left(\frac{\mathrm{i}\alpha}{(R_{\mathrm{s}}^{\mathrm{OUT}})^2}+\frac{1}{(R_{\mathrm{s}}^{\mathrm{OUT}})^3}\right)\mathrm{d}z'\,\mathrm{d}\theta', \qquad (3)
\end{aligned}$$

where

$$\begin{aligned}
R_{\mathrm{p}}^{\mathrm{DSV}} &= \left[a^2+c_1^2-z^2-2a\sqrt{c_1^2-z^2}\cos(\theta'-\theta)+(z'-z)^2\right]^{1/2},\\
R_{\mathrm{s}}^{\mathrm{DSV}} &= \left[b^2+c_1^2-z^2-2b\sqrt{c_1^2-z^2}\cos(\theta'-\theta)+(z'-z)^2\right]^{1/2},\\
R_{\mathrm{p}}^{\mathrm{OUT}} &= \left[a^2+c_2^2-z^2-2ac_2\cos(\theta'-\theta)+(z'-z)^2\right]^{1/2},\\
R_{\mathrm{s}}^{\mathrm{OUT}} &= \left[b^2+c_2^2-z^2-2bc_2\cos(\theta'-\theta)+(z'-z)^2\right]^{1/2}.
\end{aligned}$$

Considering the current continuity equation $\nabla\cdot\boldsymbol{j}(\boldsymbol{r}')=0$, we know that $j_\theta^{\mathrm{P}}(\theta',z')$ and $j_z^{\mathrm{P}}(\theta',z')$ are related to a stream function $\Psi^{\mathrm{P}}(\theta',z')$[26]

$$j_\theta^{\mathrm{P}}(\theta',z') = \frac{\partial\Psi^{\mathrm{P}}(\theta',z')}{\partial z'}, \quad j_z^{\mathrm{P}}(\theta',z') = -\frac{1}{a}\frac{\partial\Psi^{\mathrm{P}}(\theta',z')}{\partial\theta'}.$$

In order to obtain the phased array, the cylindrical surface is divided into $K\times Q$ subregions in θ' and z', respectively. The current densities in different subregions must be independent, and $j_\theta(\theta',z')$ and $j_z(\theta',z')$ must fall to zero at each boundary of θ' and z', respectively. The components of current density of the primary coil in each subregion are expanded into Fourier series

$$\begin{aligned}
j_z^{\mathrm{P}}(\theta',z') &= -\sum_{n=1}^{N}\sum_{m=1}^{M}\frac{mK}{2a}c_{mn}^{kq}\sin\left(\frac{nQ\pi(z'+L)}{2L}\right)\\
&\quad\times\cos\left(\frac{mK\theta'}{2}\right), \qquad (4)\\
j_\theta^{\mathrm{P}}(\theta',z') &= \sum_{n=1}^{N}\sum_{m=1}^{M}\frac{nQ\pi}{2L}c_{mn}^{kq}\cos\left(\frac{nQ\pi(z'+L)}{2L}\right)\\
&\quad\times\sin\left(\frac{mK\theta'}{2}\right), \qquad (5)
\end{aligned}$$

where M and N are the Fourier series terms, and the corresponding stream function is

$$\begin{aligned}
\Psi^{\mathrm{P}}(\theta',z') &= \sum_{n=1}^{N}\sum_{m=1}^{M}c_{mn}^{kq}\sin\left(\frac{nQ\pi(z'+L)}{2L}\right)\\
&\quad\times\sin\left(\frac{mK\theta'}{2}\right), \qquad (6)
\end{aligned}$$

with $k=1:K$, $q=1:Q$, $-L+(q-1)\frac{2L}{Q}\le z'\le -L+q\frac{2L}{Q}$, and $(k-1)\frac{2\pi}{K}\le\theta'\le k\frac{2\pi}{K}$.

As for the shield coil, the components of current density are the same as those of the primary coil except that a is substituted by b and L is substituted by sL. The corresponding stream function is

$$\Psi^{\mathrm{S}}(\theta',z') = \sum_{n=1}^{N}\sum_{m=1}^{M}d_{mn}^{kq}\sin\left(\frac{nQ\pi(z'+sL)}{2sL}\right)$$

$$\times \sin\left(\frac{mK\theta'}{2}\right), \tag{7}$$

with $k=1:K$, $q=1:Q$, $-sL+(q-1)\frac{2L}{Q} \le z' \le -sL+q\frac{2L}{Q}$, and $(k-1)\frac{2\pi}{K} \le \theta' \le k\frac{2\pi}{K}$.

With Eqs. (4) and (5), equations (2) and (3) can be written as

$$H_y^{\mathrm{DSV}}(\theta,z) = \sum_{q=1}^{Q}\sum_{k=1}^{K}\sum_{m=1}^{M}\sum_{n=1}^{N}\left[c_{mn}^{kq}U_{mn}^{kq}(\theta,z)+d_{mn}^{kq}V_{mn}^{kq}(\theta,z)\right], \tag{8}$$

$$H_y^{\mathrm{OUT}}(\theta,z) = \sum_{q=1}^{Q}\sum_{k=1}^{K}\sum_{m=1}^{M}\sum_{n=1}^{N}\left[c_{mn}^{kq}S_{mn}^{kq}(\theta,z)+d_{mn}^{kq}T_{mn}^{kq}(\theta,z)\right], \tag{9}$$

where

$$\begin{aligned}
&U_{mn}^{kq}(\theta,z)\\
&= -\frac{a}{2\pi}\int_{(k-1)\frac{2\pi}{K}}^{k\frac{2\pi}{K}}\int_{-L+(q-1)\frac{2L}{Q}}^{-L+q\frac{2L}{Q}}\left\{(a\cos\theta'-\sqrt{c_1^2-z^2}\cos\theta)\right.\\
&\times\left[-\frac{mK}{2a}\cos\left(\frac{mK\theta'}{2}\right)\sin\left(\frac{nQ\pi(z'+L)}{2L}\right)\right]\\
&+(z'-z)\sin\theta'\\
&\times\left.\left[\frac{nQ\pi}{2L}\cos\left(\frac{nQ\pi(z'+L)}{2L}\right)\sin\left(\frac{mK\theta'}{2}\right)\right]\right\}\mathrm{e}^{-\mathrm{i}\alpha R_{\mathrm{p}}^{\mathrm{DSV}}}\\
&\times\left(\frac{\mathrm{i}\alpha}{(R_{\mathrm{p}}^{\mathrm{DSV}})^2}+\frac{1}{(R_{\mathrm{p}}^{\mathrm{DSV}})^3}\right)\mathrm{d}z'\,\mathrm{d}\theta',
\end{aligned} \tag{10}$$

$$\begin{aligned}
&V_{mn}^{kq}(\theta,z)\\
&= -\frac{b}{2\pi}\int_{(k-1)\frac{2\pi}{K}}^{k\frac{2\pi}{K}}\int_{-sL+(q-1)\frac{2L}{Q}}^{-sL+q\frac{2L}{Q}}\left\{\left(b\cos\theta'-\sqrt{c_1^2-z^2}\cos\theta\right)\right.\\
&\left[-\frac{mK}{2b}\cos\left(\frac{mK\theta'}{2}\right)\sin\left(\frac{nQ\pi(z'+sL)}{2sL}\right)\right]\\
&+(z'-z)\sin\theta'\\
&\times\left.\left[\frac{nQ\pi}{2sL}\cos\left(\frac{nQ\pi(z'+sL)}{2sL}\right)\sin\left(\frac{mK\theta'}{2}\right)\right]\right\}\mathrm{e}^{-\mathrm{i}\alpha R_{\mathrm{s}}^{\mathrm{DSV}}}\\
&\times\left(\frac{\mathrm{i}\alpha}{(R_{\mathrm{s}}^{\mathrm{DSV}})^2}+\frac{1}{(R_{\mathrm{s}}^{\mathrm{DSV}})^3}\right)\mathrm{d}z'\,\mathrm{d}\theta',
\end{aligned} \tag{11}$$

$$\begin{aligned}
&S_{mn}^{kq}(\theta,z)\\
&= -\frac{a}{2\pi}\int_{(k-1)\frac{2\pi}{K}}^{k\frac{2\pi}{K}}\int_{-L+(q-1)\frac{2L}{Q}}^{-L+q\frac{2L}{Q}}\left\{(a\cos\theta'-c_2\cos\theta)\right.\\
&\times\left[-\frac{mK}{2a}\cos\left(\frac{mK\theta'}{2}\right)\sin\left(\frac{nQ\pi(z'+L)}{2L}\right)\right]\\
&+(z'-z)\sin\theta'\\
&\times\left.\left[\frac{nQ\pi}{2L}\cos\left(\frac{nQ\pi(z'+L)}{2L}\right)\sin\left(\frac{mK\theta'}{2}\right)\right]\right\}\mathrm{e}^{-\mathrm{i}\alpha R_{\mathrm{p}}^{\mathrm{OUT}}}\\
&\times\left(\frac{\mathrm{i}\alpha}{(R_{\mathrm{p}}^{\mathrm{OUT}})^2}+\frac{1}{(R_{\mathrm{p}}^{\mathrm{OUT}})^3}\right)\mathrm{d}z'\,\mathrm{d}\theta',
\end{aligned} \tag{12}$$

$$\begin{aligned}
&T_{mn}^{kq}(\theta,z)\\
&= -\frac{b}{2\pi}\int_{(k-1)\frac{2\pi}{K}}^{k\frac{2\pi}{K}}\int_{-sL+(q-1)\frac{2L}{Q}}^{-sL+q\frac{2L}{Q}}\left\{(b\cos\theta'-c_2\cos\theta)\right.\\
&\times\left[-\frac{mK}{2b}\cos\left(\frac{mK\theta'}{2}\right)\sin\left(\frac{nQ\pi(z'+sL)}{2sL}\right)\right]\\
&+(z'-z)\sin\theta'\\
&\times\left.\left[\frac{nQ\pi}{2sL}\cos\left(\frac{nQ\pi(z'+sL)}{2sL}\right)\sin\left(\frac{mK\theta'}{2}\right)\right]\right\}\mathrm{e}^{-\mathrm{i}\alpha R_{\mathrm{s}}^{\mathrm{DSV}}}\\
&\times\left(\frac{\mathrm{i}\alpha}{(R_{\mathrm{s}}^{\mathrm{DSV}})^2}+\frac{1}{(R_{\mathrm{s}}^{\mathrm{DSV}})^3}\right)\mathrm{d}z'\,\mathrm{d}\theta'.
\end{aligned} \tag{13}$$

The magnetic field is required to be homogeneous in the DSV and zero in the OUT. Suppose the numbers of selected points in the DSV and the OUT are D_{P} and O_{P}, respectively, then the error between induced and desired magnetic fields of the sampling points can be noted as

$$\Phi = \sum_{i=1}^{D_{\mathrm{P}}}\sum_{j=1}^{O_{\mathrm{P}}}\left[\left(H_{y,i}^{\mathrm{DSV}}-H_{\mathrm{yT},i}^{\mathrm{DSV}}\right)^2+\left(H_{y,j}^{\mathrm{OUT}}-H_{\mathrm{yT},j}^{\mathrm{OUT}}\right)^2\right], \tag{14}$$

where $H_{y,i}^{\mathrm{DSV}}$ and $H_{y,j}^{\mathrm{OUT}}$ refer to magnetic fields of sampling points in the DSV and the OUT, respectively; $H_{\mathrm{yT},i}^{\mathrm{DSV}}$ and $H_{\mathrm{yT},j}^{\mathrm{OUT}}$ refer to target magnetic fields of sampling points in the DSV and the OUT, respectively. To minimize the error between induced and desired magnetic fields of sampling points, let the derivatives of Eq. (14) with respect to c_{mn}^{kq} and d_{mn}^{kq} be zero, that is

$$\frac{\partial\Phi}{\partial c_{mn}^{kq}}=0, \quad \frac{\partial\Phi}{\partial d_{mn}^{kq}}=0. \tag{15}$$

Equation (15) can be rewritten as

$$\begin{aligned}
&\sum_{q=1}^{Q}\sum_{k=1}^{K}\sum_{m=1}^{M}\sum_{n=1}^{N}\left\{\sum_{i=1}^{D_{\mathrm{P}}}c_1U_{mn}^{kq}(\theta,z)[c_{mn}^{kq}U_{mn}^{kq}(\theta,z)\right.\\
&+d_{mn}^{kq}V_{mn}^{kq}(\theta,z)]\\
&+\left.\sum_{i=1}^{O_{\mathrm{P}}}c_2S_{mn}^{kq}(\theta,z)\left[c_{mn}^{kq}S_{mn}^{kq}(\theta,z)+d_{mn}^{kq}T_{mn}^{kq}(\theta,z)\right]\right\}\\
&=\sum_{q=1}^{Q}\sum_{k=1}^{K}\sum_{m=1}^{M}\sum_{n=1}^{N}\left[\sum_{i=1}^{D_{\mathrm{P}}}c_1U_{mn}^{kq}(\theta,z)H_{\mathrm{yT},i}^{\mathrm{DSV}}\right],
\end{aligned} \tag{16}$$

$$\begin{aligned}
&\sum_{q=1}^{Q}\sum_{k=1}^{K}\sum_{m=1}^{M}\sum_{n=1}^{N}\left\{\sum_{i=1}^{D_{\mathrm{P}}}c_1V_{mn}^{kq}(\theta,z)[c_{mn}^{kq}U_{mn}^{kq}(\theta,z)\right.\\
&+d_{mn}^{kq}V_{mn}^{kq}(\theta,z)]\\
&\times\left.\sum_{i=1}^{O_{\mathrm{P}}}c_2T_{mn}^{kq}(\theta,z)\left[c_{mn}^{kq}S_{mn}^{kq}(\theta,z)+d_{mn}^{kq}T_{mn}^{kq}(\theta,z)\right]\right\}\\
&=\sum_{q=1}^{Q}\sum_{k=1}^{K}\sum_{m=1}^{M}\sum_{n=1}^{N}\left[\sum_{i=1}^{D_{\mathrm{P}}}c_1V_{mn}^{kq}(\theta,z)H_{\mathrm{yT},i}^{\mathrm{DSV}}\right].
\end{aligned} \tag{17}$$

Equations (16) and (17) can be represented as a series of linear equations, which is expressed in a matrix form

$$\boldsymbol{AX}=\boldsymbol{T}, \tag{18}$$

where the coefficients c_{mn}^{kq} and d_{mn}^{kq} are stored in the vector $\boldsymbol{X}$, the elements in square matrix $\boldsymbol{A}$ can be obtained from Eqs. (10)–(13) using the double Gauss integral. The highly

ill-conditioned nature of matrix $\boldsymbol{A}$ generally results in gross inaccuracies in the solution. To solve this problem, a regularization strategy (Tikhonov regularization) is implemented. A penalty function P related to the minimum curvature is added to Φ to produce a residual error Φ'

$$\Phi' = \Phi + \lambda P, \tag{19}$$

where λ is the penalty factor (also called the Tikhonov regularization factor), and

$$\begin{aligned} P = {} & a\sum_{q=1}^{Q}\sum_{k=1}^{K}\int_{-L+(q-1)\frac{2L}{Q}}^{-L+q\frac{2L}{Q}}\int_{(k-1)\frac{2\pi}{K}}^{k\frac{2\pi}{K}}\left[\left(\nabla^2 j_\theta^{\mathrm{P}}\right)^2\right. \\ & \left.+\left(\nabla^2 j_z^{\mathrm{P}}\right)^2\right]\mathrm{d}\theta'\mathrm{d}z' \\ & +b\sum_{q=1}^{Q}\sum_{k=1}^{K}\int_{-sL+(q-1)\frac{2L}{Q}}^{-sL+q\frac{2L}{Q}}\int_{(k-1)\frac{2\pi}{K}}^{k\frac{2\pi}{K}}\left[\left(\nabla^2 j_\theta^{S}\right)^2\right. \\ & \left.+\left(\nabla^2 j_z^{S}\right)^2\right]\mathrm{d}\theta'\mathrm{d}z'. \end{aligned} \tag{20}$$

By substituting the components of current density of both primary and shield coils, Eq. (20) can be written as

$$\begin{aligned} P = {} & \sum_{q=1}^{Q}\sum_{k=1}^{K}\sum_{m=1}^{M}\sum_{n=1}^{N}\left\{\frac{a\pi L}{KQ}\left(c_{mn}^{kq}\right)^2\left[\left(\frac{mK}{2a}\right)^2+\left(\frac{nQ\pi}{2L}\right)^2\right]^3\right. \\ & \left.+\frac{b\pi sL}{KQ}\left(d_{mn}^{kq}\right)^2\left[\left(\frac{mK}{2b}\right)^2+\left(\frac{nQ\pi}{2sL}\right)^2\right]^3\right\}. \end{aligned} \tag{21}$$

Minimizing Φ' with respect to c_{mn}^{kq} and d_{mn}^{kq} gives a new series of linear equations, which can be expressed in the matrix form as

$$(\boldsymbol{A}+\lambda\boldsymbol{\Gamma})\,\boldsymbol{X} = \boldsymbol{T}, \tag{22}$$

where $\boldsymbol{\Gamma}$ is a diagonal matrix, which contains the minimum condition related to Eq. (21).

After the coefficients c_{mn}^{kq} and d_{mn}^{kq} are solved, the coil windings of the primary and the shield coils can be obtained via contouring the stream function $\Psi^{kq}(\theta',z')$ in Eqs. (6) and (7). To get a static winding pattern, the time average of the stream function $\Psi^{\mathrm{P}}(\theta',z')$ in Eq. (6) should be taken as

$$\Psi\left(\theta',z'\right) = \frac{\omega}{2\pi}\int_0^{\frac{2\pi}{\omega}}\left\|\Psi^{\mathrm{P}}\left(\theta',z'\right)\Psi^{P*}\left(\theta',z'\right)\right\|, \tag{23}$$

here $\Psi^{P*}(\theta',z')$ is the complex conjugate of $\Psi^{\mathrm{P}}(\theta',z')$. The time average of the stream function $\Psi^{\mathrm{S}}(\theta',z')$ in Eq. (7) is the same as $\Psi(\theta',z')$ in Eq. (23) except that P is replaced by S.

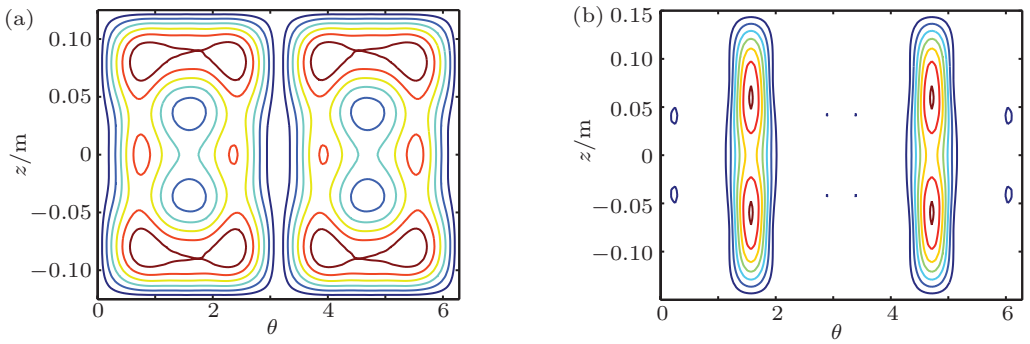
After the stream function is discretized, the magnetic field in the DSV (or OUT) can be re-calculated by using the Biot–Savart integral equation, and the error between magnetic and target fields can be evaluated.

3. Results

3.1. Shielded phased array of $K \times Q = 2 \times 1$

Firstly, a shielded 2×1 array is considered. The dimensions of the primary RF coil are chosen to be $L = 0.125$ m, $a = 0.1$ m, and the radius of the DSV is $c = 0.05$ m. The shield coil is taken to have radius $b = 0.125$ m and parameter $s = 1.2$. The cylindrical target region exterior to the shield coil is taken to be of radius $c_2 = 0.15$ m and parameter $t = 0.9$. The desired magnetic field is $H_{y\mathrm{T}}^{\mathrm{DSV}} = 1$ A/m in the DSV and $H_{y\mathrm{T}}^{\mathrm{OUT}} = 0$ in the OUT. The Larmor frequency is taken to be 190 MHz, which is corresponding to a static magnetic field of 4.5 T. In the design, 121 points in the DSV and the OUT are selected respectively. The Fourier series terms in the program are taken to be $M = N = 9$. The condition number of matrix $\boldsymbol{A}$ is found to be 2.28×10^{19}, while the condition number of diagonal matrix $\boldsymbol{\Gamma}$ is 1.16×10^{6}.

The condition number of matrix $\boldsymbol{A} + \lambda\boldsymbol{\Gamma}$ varies with penalty factor λ and is listed in Table 1. It reduces from 5.79×10^{14} to a minimum of 8.05×10^{4} with the increase of λ, and then increases due to the effect of matrix $\boldsymbol{\Gamma}$. For three penalty factors ($\lambda = 10^{-10}, 10^{-9}, 10^{-6}$), the winding patterns of coils and the errors between induced and target fields in the DSV and the OUT are shown in Fig. 2.



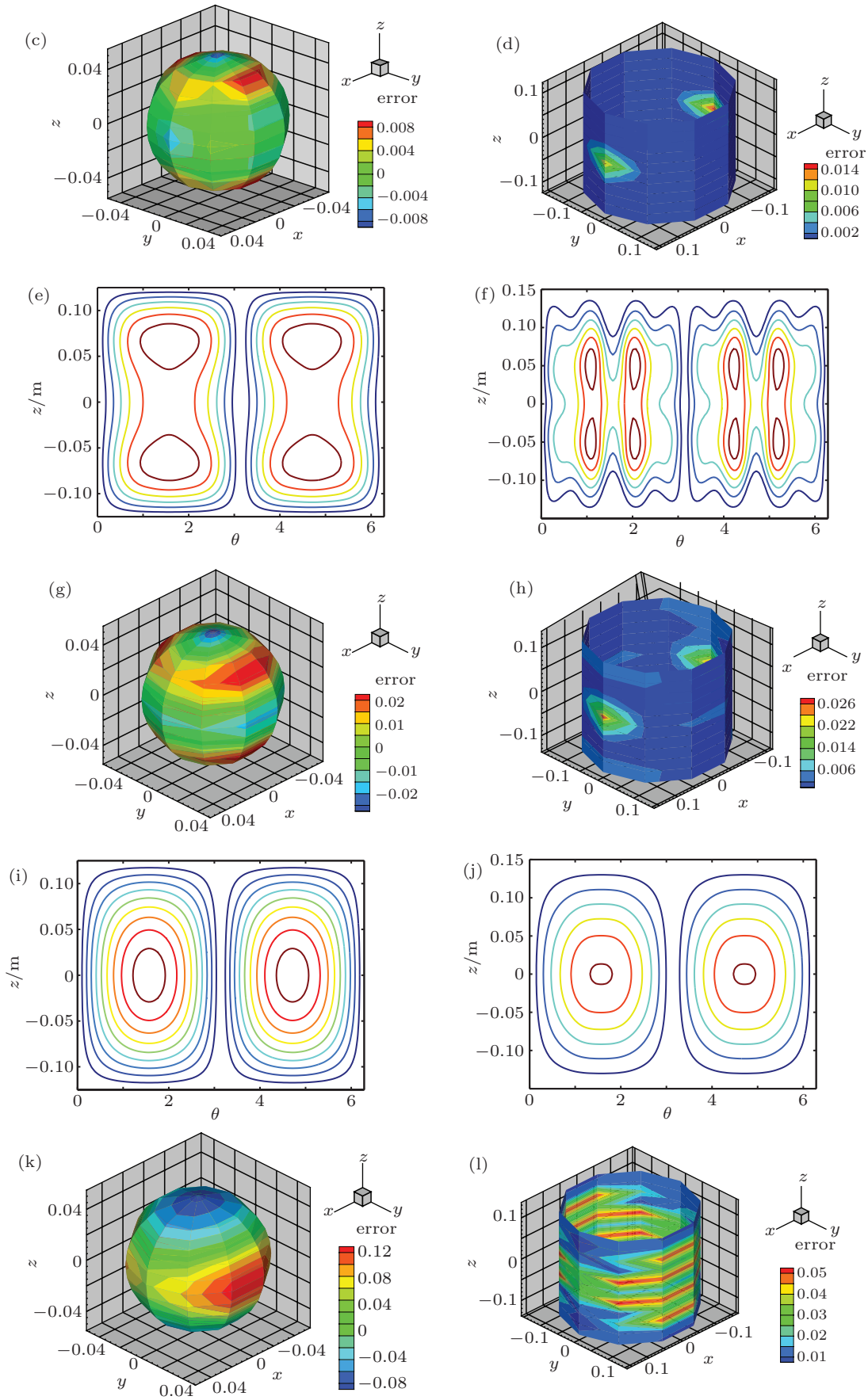


Fig. 2. (color online) The winding patterns of primary and shield coils and the errors in the DSV and the OUT for (a)–(d) $\lambda = 10^{-10}$, (e)–(h) $\lambda = 10^{-9}$, and (i)–(l) $\lambda = 10^{-6}$.

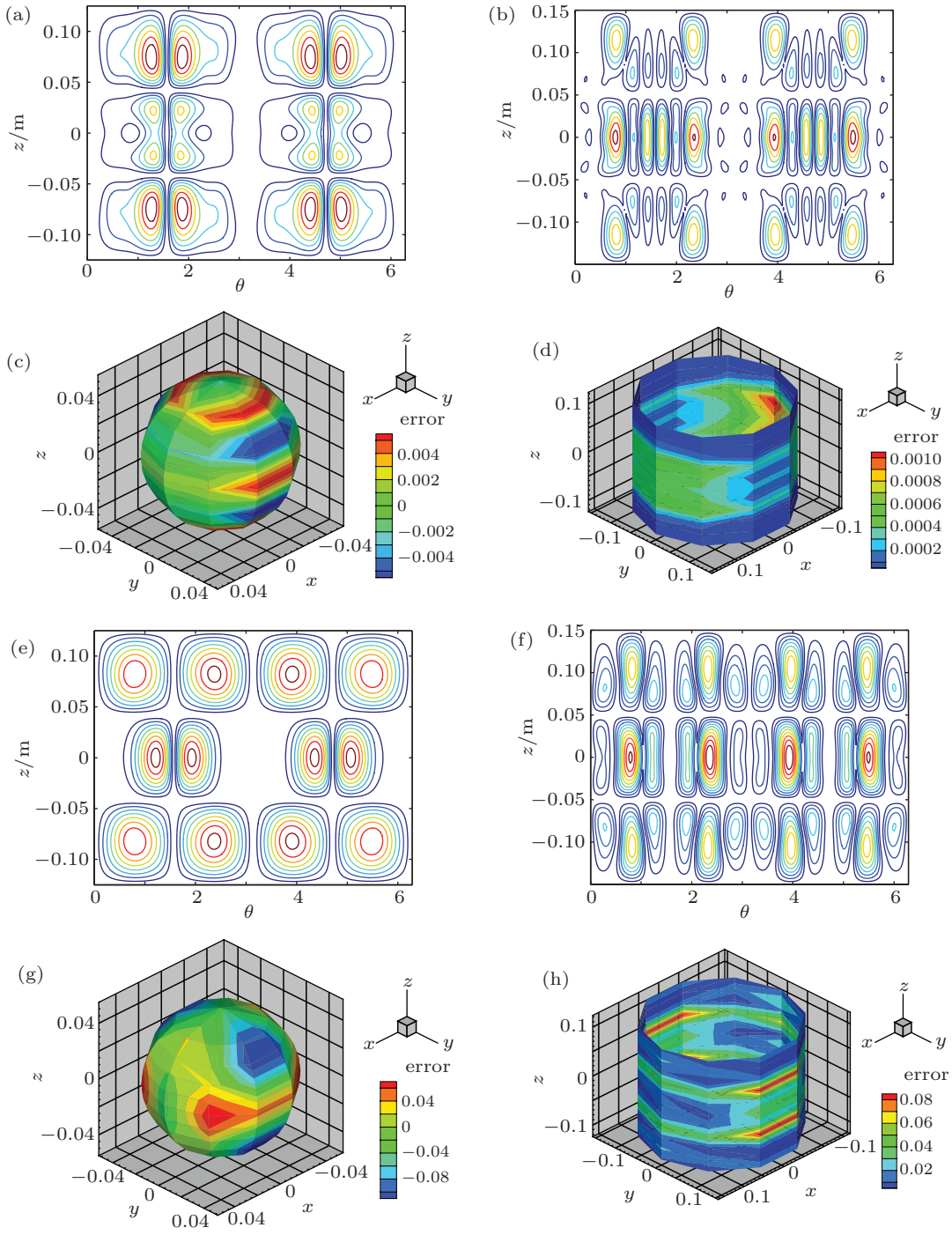
Table 1. Condition number of matrix $\boldsymbol{A}+\lambda\boldsymbol{\Gamma}$ for 2×1 shielded array.

λ	10^{-19}	10^{-16}	10^{-10}
cond$(\boldsymbol{A}+\lambda\boldsymbol{\Gamma})$	5.79×10^{14}	5.86×10^{11}	8.86×10^{5}
λ	10^{-9}	10^{-6}	10^{-4}
cond$(\boldsymbol{A}+\lambda\boldsymbol{\Gamma})$	9.55×10^{4}	8.05×10^{4}	6.39×10^{5}

When $\lambda=10^{-10}$, the magnetic field is highly homogeneous in the DSV and nearly zero in the OUT. With the increase of λ, the errors of the magnetic fields in the DSV and the OUT become bigger, and simpler and smoother winding patterns are obtained. So there is a trade-off between coil array simplicity and magnetic homogeneity.

3.2. Shielded phased array of $K\times Q=4\times3$

A 4×3 coil array is also discussed in this paper, the geometries of which are the same as those of the 2×1 array discussed above. The condition number of matrix $\boldsymbol{A}$ is found to be 6.41×10^{22}, while the condition number of diagonal matrix $\boldsymbol{\Gamma}$ is 1.11×10^{6}. With the increase of λ, the condition number of matrix $\boldsymbol{A}+\lambda\boldsymbol{\Gamma}$ reduces from 1.97×10^{13} to a minimum of 2.28×10^{5} and then increases due to the effect of matrix $\boldsymbol{\Gamma}$. For three penalty factors ($\lambda=10^{-12},10^{-9},10^{-6}$), the winding patterns of coils and the errors between induced and target fields in the DSV and the OUT are shown in Fig. 3.



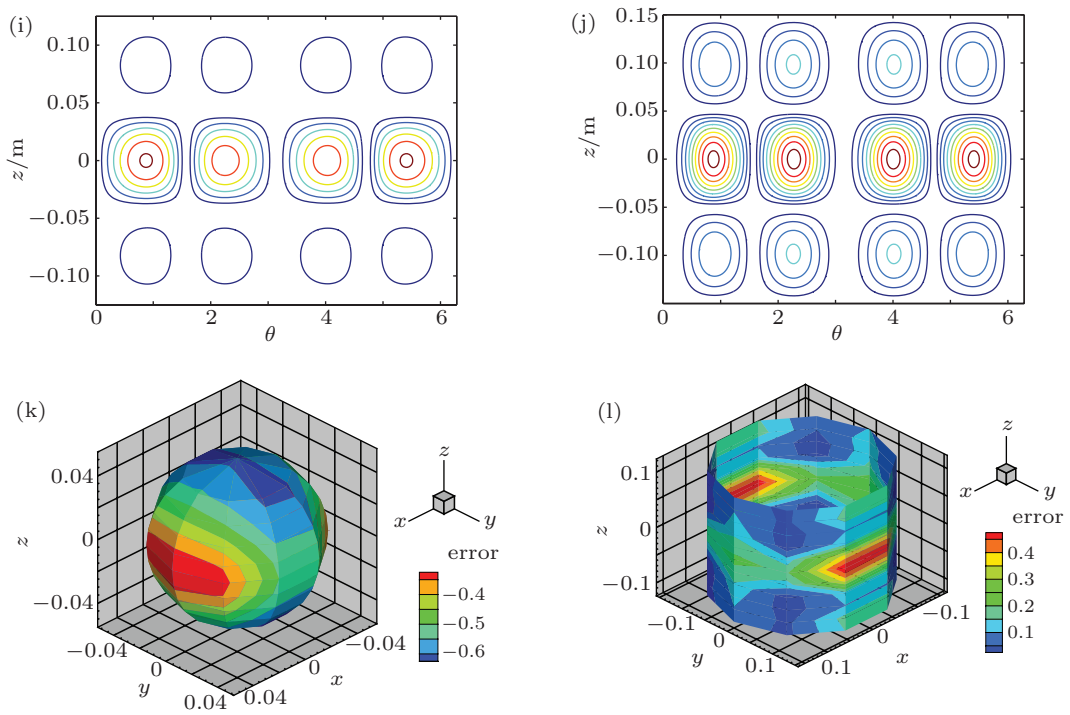


Fig. 3. (color online) The winding patterns of primary and shield coils and the errors in the DSV and the OUT for (a)–(d) $\lambda = 10^{-12}$, (e)–(h) $\lambda = 10^{-9}$, and (i)–(l) $\lambda = 10^{-6}$.

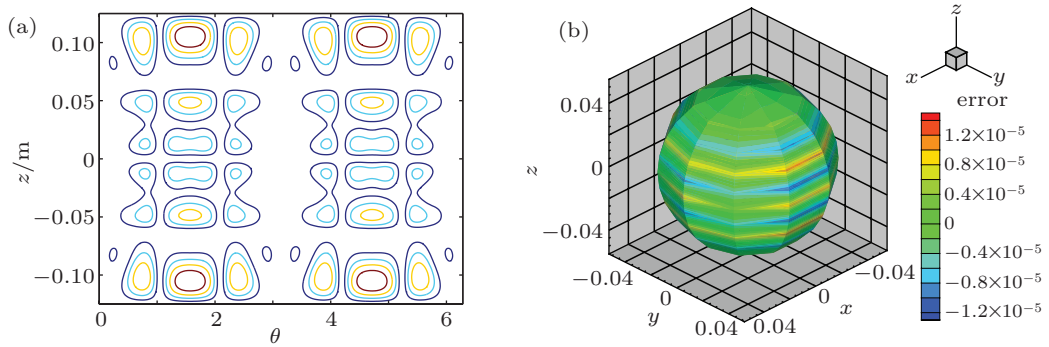
3.3. Unshielded phased array of $K \times Q = 6 \times 4$

A 6×4 unshielded phased array which contains only the primary coil is also considered. The dimensions of the RF coil are chosen to be the same as those of the primary coil. Similar to the design of shielded RF coils, the change of condition number of matrix $\boldsymbol{A} + \lambda \boldsymbol{\Gamma}$ is listed in Table 2.

The coils and the errors corresponding to selected λ are shown in Fig. 4. When λ is smaller than 10^{-16}, the winding patterns are much more complicated. The winding patterns are smoother and simpler for $\lambda = 10^{-9}$ than those for $\lambda = 10^{-16}$ due to the effect of the penalty factor. Though little change appears between the condition numbers of matrix $\boldsymbol{A} + \lambda \boldsymbol{\Gamma}$ for $\lambda = 10^{-9}$ and $\lambda = 10^{-7}$, the error between induced and target fields increases obviously.

Table 2. Condition number of matrix $\boldsymbol{A} + \lambda \boldsymbol{\Gamma}$ for 6×4 unshielded array.

λ	10^{-23}	10^{-16}	10^{-11}
cond$(\boldsymbol{A} + \lambda \boldsymbol{\Gamma})$	5.79×10^{17}	1.44×10^{10}	4.40×10^{5}
λ	10^{-9}	10^{-7}	
cond$(\boldsymbol{A} + \lambda \boldsymbol{\Gamma})$	5.28×10^{5}	5.31×10^{5}	



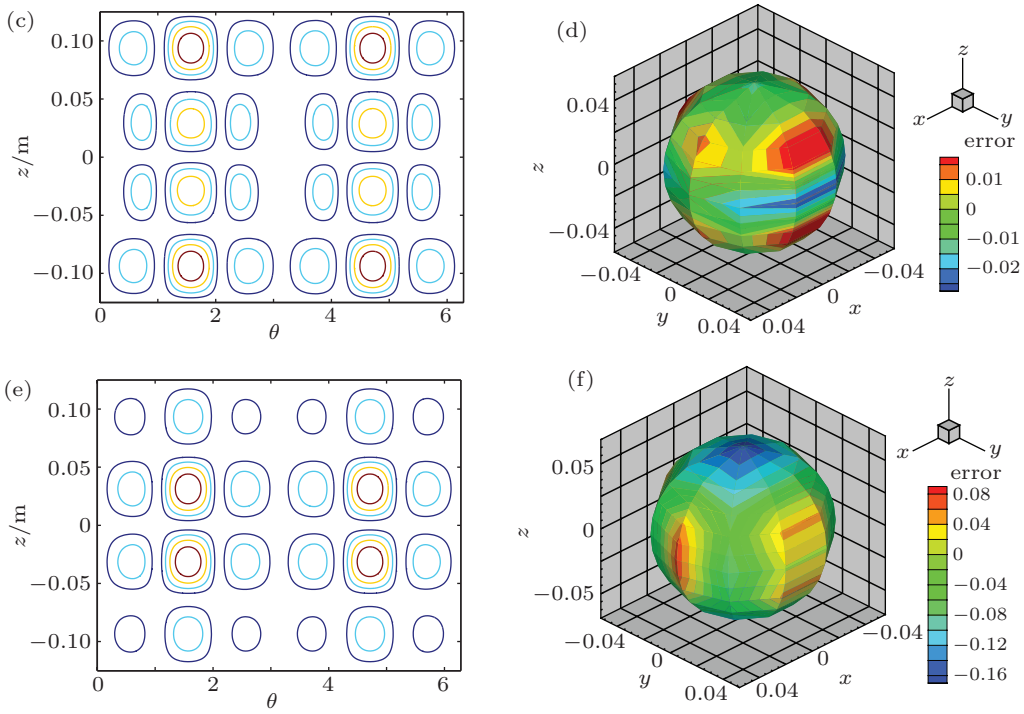


Fig. 4. (color online) The winding patterns of coils and the errors in the DSV for (a), (b) $\lambda = 10^{-16}$; (c), (d) $\lambda = 10^{-9}$; and (e), (f) $\lambda = 10^{-7}$.

4. Conclusion

An approach to the design of an actively shielded phased-array coil system is proposed in this paper. The current densities of RF coils are expended into the Fourier series, and the highly ill-conditioned nature of the inverse method is resolved by the Tikhonov regularization with the minimum curvature penalty function. It is found that there is a trade-off between coil array simplicity and magnetic field homogeneity with the choice of penalty factor. Results show that with the increase of penalty factor λ, the condition number of matrix $\boldsymbol{A} + \lambda \boldsymbol{\Gamma}$ reduces to a minimum and then increases due to the effect of matrix $\boldsymbol{\Gamma}$, which means that the accuracy of the solution of the Fourier series increases and then reduces. At the same time, the winding patterns can become simpler and smoother with the increase of penalty factor. A compromise between coil array simplicity and magnetic field homogeneity can be reached with an appropriate selection of penalty factor.

References

[1] Zu D L, Guo H, Song X Y and Bao S L 2002 *Chin. Phys.* B **11** 1008
[2] Tang X, Hong L M and Zu D L 2010 *Chin. Phys.* B **19** 078702
[3] Jin J M1999 *Electromagnetic Analysis and Design in Magnetic Resonance Imaging* (Boca Raton: CRC Press)
[4] Meng B, Huang K W and Wang W M 2010 *Chin. Phys.* B **19** 076103
[5] Turner R 1986 *J. Phys.* D: *Appl. Phys.* **19** 147
[6] Fobes L K, Crozier S and Doddrell D M 1997 *SIAM J. Appl. Math.* **57** 401
[7] Lawrence B G, Crozier S and Yau D D 2002 *IEEE Trans. Biomed. Eng.* **49** 64
[8] While P T, Forbes L K and Crozier S 2005 *Meas. Sci. Technol.* **16** 997
[9] Cui K and Yang G W 2005 *Chin. Phys. Lett.* **22** 2738
[10] Tang F K, Hua N, Tang X Z, Lu H, Wang Q and Ma P 2010 *Chin. Phys.* B **19** 120601
[11] Hua N, Tang X Z, Lu H, Tang F K, Wang Q and Ma P 2010 *Chin. Phys.* B **19** 080601
[12] Hua S X and Zhao X F 2011 *Chin. Phys.* B **20** 029201
[13] Liu W T, Zu D L and Tang X 2010 *Chin. Phys.* B **19** 018701
[14] Zhao X F and Huang S X 2011 *Acta Phys. Sin.* **60** 119203 (in Chinese)
[15] Zhou J M, Wang H N and Yao J J 2012 *Acta Phys. Sin.* **61** 089101 (in Chinese)
[16] Ding G T 2011 *Acta Phys. Sin.* **60** 044503 (in Chinese)
[17] Hoult D I and Deslauriers R 1994 *J. Magn. Reson. Ser.* A **108** 9
[18] Elaine A C and Brian K R 1998 *Magn. Reson. Med.* **39** 270
[19] Li Y, Liu F and Weber E 2009 *Concepts Magn. Reson.* **35B** 221
[20] Martens M A, Petropoulos L S and Brown R W 1991 *Rev. Sci. Instrum.* **62** 2639
[21] While P T, Forbes L K and Crozier S 2005 *Meas. Sci. Technol.* **16** 1381
[22] Jasinski K, Mlynarczyk A, Latta P, Volotovskyy V, Weglarz W P and Tomanek B 2012 *Magn. Reson. Imaging* **30** 70
[23] Roemer P B, Edelstein W A, Hayes C E, Souza S P and Mueller O M 1990 *Magn. Reson. Med.* **16** 192
[24] Wu B, Wang C S, Douglas A C K, Xu D, Vigneron D B, Nelson S J and Zhang X L 2010 *IEEE Trans. Med. Imaging* **29** 179
[25] While P T, Forbes L K and Crozier S 2007 *Meas. Sci. Technol.* **18** 245
[26] Alan E W, Frederick S J and Abdulhassain H M (European Patent) 0140259 [1985-05-08]